Conf-9410314--2

UCRL-JC-119309
PREPRINT

Observation on Radiation Transfer Experiments Using k-Shell Absorption Spectra

C. A. Iglesias
M. H. Chen
D. L. McWilliams
J. K. Nash
F. J. Rogers

This paper was prepared for submittal to the
6th International Workshop on Radiative
Properties of Hot Dense Matter

October 31-November 4, 1994
Sarasota, Florida

January 4, 1995

Lawrence Livermore National Laboratory

DISCLAIMER

DISCLAIMER

Portions of this document may be illegible in electronic image products. Images are produced from the best available original document.

OBSERVATIONS ON RADIATION TRANSFER EXPERIMENTS USING *K*-SHELL ABSORPTION SPECTRA

C. A. IGLESIAS, M. H. CHEN, D. L. MCWILLIAMS, J. K. NASH, AND F. J. ROGERS
Lawrence Livermore National Laboratory
P. O. Box 808, Livermore, CA 94550

ABSTRACT - Recent laser-produced plasma experiments have relied on spectroscopic comparisons with models to infer plasma temperatures. Here, the technique is applied to study thermal radiation transfer experiments. The transmission model combines high-quality atomic data with an ionization balance obtained from systematic expansions of the grand canonical ensemble. The latter avoids the *ad hoc* cutoffs required in free energy minimization schemes and includes Coulomb corrections usually neglected in other models. It is shown that the improved equation of state significantly affects inferred temperatures at the higher densities expected in the heat flow experiments. Even though good agreement is obtained between the experimental and theoretical transmission spectrum, the experimental uncertainties are sufficiently large that it compromises the intended bench marking of the thermal transport models.

Prepared for the Proceedings of the
6th International Workshop on the Radiative Properties of Hot Dense Matter,
Sarasota, Fl., Oct 31-Nov.4, 1994.

1. INTRODUCTION

The radiative properties of hot, dense matter have long been of interest in astrophysics and laboratory plasmas. Although the interpretation of photon absorption in plasmas has proven difficult, recent efforts have yielded valuable information.[1-4] The success has been due, in part, to the production of plasmas that are uniform, reproducible, and near local thermodynamic equilibrium. An important hurdle was overcome with the development of techniques to determine the plasma conditions accurately. For example, the ability to infer plasma temperatures from comparisons of theoretical calculations and expermental absorption spectra was established.[1] Past experiments have concentrated on aluminum as a thermometer since its *K*-shell photoabsorption spectrum is relatively simple and involves experimentally convenient photon energies. Early experiments and model calculations were done by Davidson *et al.*[5] Later experiments[1] used a model by Abdallah and Clark.[6] More recently a third method was developed that also includes spectroscopically accurate atomic data but offers improvements in the ionization balance calculation.[7]

The present work uses the last method[7] (hereafter OPAL/MCDF) to study a radiation transfer experiment in laser-produced plasmas. The experiment was performed as a first step to develop techniques for studying radiation heat transfer.[8] Briefly, a cylindrical gold tube filled with a SiO_2 aerogel is heated from one end by an x-ray drive produced by a gold hohlraum that has been irradiated with laser beams. At the opposite end of the tube is located a thin aluminum foil. As the heating of the tube proceeds, the aluminum foil is illuminated by a broad band of x-rays produced by a small samarium fiber that has been irradiated with additional laser beams. The time dependent transmission spectra through the aluminum sample can then be compared with absorption calculations to infer the aluminum sample conditions. It is hoped that such studies can help evaluate the predictive capabilities of codes used to model the time dependent transfer of heat by radiation.

2. METHOD

One requirement of theoretical calculations for comparison with experimental spectra is extraordinary fidelity in the wavelengths. In the present work, line energies and oscillator strengths are calculated using the relativistic configuration interaction method.[9,10] For each ionization stage, the states from the following configurations are included in the calculations:

$1s^2 2l^m$ and $1s^2 2l^{m-1} n'l'$

as well as

$1s 2l^{m+1}$ and $1s 2l^m n'l'$

for all $3 \leq n' \leq 7$ and $l' < n'$. To minimize the size of the calculation, only states with $n' \leq 4$ are included in the same basis set expansion. For states with $n' \geq 5$ separate calculations are performed for each n'. The orbital wave functions are computed using the Dirac-Hartree-Slater method[11] and include the Breit interaction, quantum electrodynamics corrections, and finite nuclear size effects. The computed *1s* to *2p* transition energies of partially ionized aluminum are reasonably accurate; that is, approximately 1 eV or less uncertainty. These errors are mostly due to the residual electron correlation effects.

The ionization balance is based on systematic expansions of the grand canonical partition function[12] that avoid the *ad hoc* cutoffs necessary in free energy minimization schemes.[5,6] The cutoffs in the latter approaches are used to truncate the internal partition function,

$$\sum_j g_j \exp(-E_j / T) \propto N^3 \qquad (1)$$

where the sum is over bound levels, g_j is the degeneracy of level j, E_j is its energy, and T is the temperature in energy units. Equation (1) diverges as N^3 where N is the largest principal quantum number included in the sum. Typically, models assume a maximum N based on heuristic arguments, or equivalently, a short-ranged potential that restricts the sum. No cutoff is necessary in the activity expansion approach since performing the complete trace,[12] including both bound and scattering states, removes the divergence in Eq.(1). The ionization balance also includes Coulomb interaction terms neglected in Refs. 5 and 6. The lowest order term is the well-known Debye-Hückel correction to the ideal gas pressure or free energy, but higher orders are also retained.

The line shapes and other necessary photoabsorption cross sections (e.g., photon ionization) are treated with the OPAL code.[13] That is, the present calculation uses the OPAL code, except that it replaces the line energies and oscillator strengths generated internally by OPAL with the more accurate results from the relativistic configuration interaction method described above. This model has been compared to aluminum experiments[7] and applied in an iron opacity measurement using fluorine and sodium *K*- and *L*-shell transitions to infer the temperature.[4]

The heating of the gold tube is simulated with a 2-D Lagrangian radiation hydrocode.[14] The heating radiation drive is represented by a Planckian source with a time-dependent radiation temperature that neglects any non-thermal components (the gold M-shell bands). The drive temperature was characterized in separate experiments and showed a shot-to-shot variation of about 10%.[8] Even though a 2 dimensional simulation of the heating was performed, the transmission calculations assumed that the aluminum foil was well represented by an annulus at one third of the tube radius. In addition, the foil was assumed uniform in density and temperature along the line of sight which is parallel to the tube axis of symmetry. Although these are obvious simplifications that could lead to errors, the model is sufficient to demonstrate that the uncertainties in the present experiments are probably too large for testing hydrocodes.

The main quantity of interest is the transmission through the aluminum foil. Experimentally the transmission is obtained by comparing the direct samarium spectrum with that attenuated by the aluminum sample. The theoretical transmission is given by

$$T(\nu) = \exp[-\rho L \kappa(\nu)] \quad (2)$$

where ρ is the mass density, $\kappa(\nu)$ the photoabsorption cross section, and L the foil thickness. Here, the hydrocode simulations are used to provide the aluminum temperature and density as input to the photoabsortion model. The resulting $\kappa(\nu)$ is then substituted into Eq. (2) and $T(\nu)$ compared to the experimental results. Obviously, the success of the analysis and any conclusions concerning the hydrodynamic simulations depends critically on the model that generates $\kappa(\nu)$ as well as the quality of the experimental data.

3. ANALYSIS

In order to make meaningful quantitative comparisons between the experimental and theoretical transmission, the experiments should meet similar criteria as in earlier opacity measurements.[1-4] For example, the aluminum sample should be reasonably close to local thermodynamic equilibrium. However, it is shown below that since the radiation drive as well as the relative timing between the start of the heating and the transmission measurements play a crucial role in the analysis, the radiation transfer experiments have complications not present in earlier opacity measurements.

3.1 MODEL UNCERTAINTIES

It is important that models used to inferred quantities from the experimental data be independently tested. Such a test was done for the temperature determination[1] by spectroscopic comparisons in earlier opacity measurements. In the radiation transfer experiments, however, the plasma densities are considerably higher and the ionization balance, which is critical for the transmission spectra calculation, is shown to be sensitive to the models.

Table 1 contains the simulated temperatures and densities for the aluminum foil as a function of time at a distance of one third the radius from the tube axis of symmetry.[14] To demonstrate the sensitivity of the absorption spectra on the ionization balance calculations at the predicted plasma conditions, results from OPAL/MCDF are compared in Fig. 1 with one that ignores the Coulomb corrections. That is, the latter models ignores contributons to the pressure from the Coulomb interactions where the lowest order term is the well known Debye-Hückle result. The significant difference in the transmission spectra is due to the Coulomb interactions which lower the pressure relative to the ideal gas result and the system compensates by increasing the number of particles. Consequently, at the same plasma conditions the two calculations yield a different ionization balance that is most pronounced in the absorption from ions in the wings of the charge state distribution.

Since the spectrum depends on the charge state distribution, reasonable agreement can be obtained between the two models by adjusting the temperature in one of them. For comparison, a calculation with OPAL/MCDF at a lower temperature is also displayed in Fig. 1. Similar calculations were repeated for the last 5 points in Table 1 and good agreement between the ideal gas model and OPAL/MCDF was obtained as in Fig. 1 by lowering the temperature in the latter by 5-7eV. Thus, the Coulomb corrections can significantly alter the inferred plasma temperatures at the densities encountered in the present experiments. In contrast, any temperature uncertainties due to the ionization balance models in previous absorption experiments[1-4] were considerably reduced since there the matter densities were about an order of magnitude smaller and the Coulomb corrections were negligible.

3.2 Experiment and Model Comparisons

Figure 2 presents comparisons between the experimental transmission and calculations with OPAL/MCDF using conditions specified in Table 1. Early times are not displayed since at the colder temperatures the aluminum *1s* to *2p* spectrum is very weak. In general, there is poor agreement between the experiment and theory. To investigate the potential error in temperature implied by the comparison in Fig. 2, two calculations with OPAL/MCDF at the same density but different temperatures are presented in Fig. 3. The improved agreement at the considerable lower temperature suggests a potential large error in the hydrodynamic calculations of the plasma conditions (much larger than the temperature uncertainties from the ionization balance models).

Note that in the comparisons in Fig. 2 and 3 the experimental results for 800 and 900ps include a 4 eV shift toward higher energies. This was done to improve line coincidence between experiment and theory at the lower end of the energy range. Such a shift is not required for the higher-energy *1s* to *2p* lines. Perhaps there are errors in the experimental energy scale determination or the atomic calculations are systematically overestimating the transition energies for the less ionized ions.

3.3 Experimental Uncertainties

As mentioned above the radiation transfer experiments are further complicated since now the radiation drive and timing issues are relevant to the transmission measurements. It is shown below that it is possible to obtain reasonable agreement between theory and experiment within the experimental uncertainties.

The experiments require synchronization between the start of the heating and the time of the transmission measurements. This timing uncertainty[15] is approximately 100ps and its effects are considered in Fig. 4. The figure compares OPAL/MCDF results and experiment, but it shifts the theoretical results to later times by 100ps. Overall there is considerable improvement in the agreement, except at 1200ps. Although for this latest time the figure shows an incorrect time shift of 200 rather than 100ps,[16] it is inconsequential since the best fit from theory is at a hotter temperature (T=92eV, ρ=0.133g/cm^3); that is, better agreement requires a time shift in the opposite direction. The discrepancies at the late times between experiment and theory could be due to oversimplification of the simulations. For example, gradients can develop both parallel and perpendicular to the line of sight that are not included here. Again, the experimental results at 800 and 900ps in Fig. 4 are shifted by 4 eV.

A second source of experimental uncertainty is the x-ray drive that heats the tube which is not measured in the same shot as the transmission and displays a shot-to-shot variation of 10% in the assumed time dependent Planckian temperature.[8] Results from hydrodynamic calculations[14] with a drive temperature scaled by 0.9 are given in Table 2 and the resulting transmission spectra form OPAL/MCDF are compared to the experiment in Fig. 5. Again, there is poor agreement between theory and experiment. As before, a 100ps time shift of the theory, but now towards earlier times, considerably improves the comparison as shown in Fig. 6. These comparisons suggest that there is a drive-temperature scaling factor between 0.9 and 1 that leads to reasonable agreement between models and experiment without invoking a time shift. The comparisons also suggest that timing and drive uncertainties are indistinguishable in this type of analysis. That is, lowering (raising) the radiation drive temperature means that it will take a longer (shorter) time for the aluminum foil to reach a given temperature which can be compensated by a time shift.

4. CONCLUSION

A recently developed model for interpreting photoabsorption measurements has been applied to radiation transfer experiments. The model has spectroscopically accurate atomic data and avoids *ad hoc* cutoffs necessary in free energy minimization schemes. It was shown that at the higher densities in this experiments the Coulomb corrections can affect the ionization balance calculations and have significant impact on the computed spectrum and inferred temperature. Unfortunately, issues concerning the ionization balance remain experimentally unresolved since there have been almost no efforts to discriminate among present theories. Astronomical observations,[17,18] however, support the necessity for the Coulomb terms included in the present approach. Future absorption experiments at higher densities that can experimentally determine both the temperature and density of the plasma may be able to address the ionization balance issues. Furthermore, due to the important contribution of satellite lines (e.g., $1s^2 2l^m n'l'$ to $1s2l^{m+1}n'l'$) to the transmission,[19] it may be possible to study many-body effects on excited bound states.

Overall there is, within the limits of experimental uncertaintity, reasonable agreement between the experiment and the transmission model using densities and temperatures from the hydrocode. However, present experimental uncertainties are large so that the comparisons do not provide significant constraints on the models. There are at least two critical sources of uncertainty in the experiment: the energy in the radiation drive heating the gold tube and timing errors in the transmission spectra. It should be emphasized that this type of experiment is relatively new and future refinements are possible. For example, several diagnostic foils could be inserted along the length of the tube that could reduce the dependence on the absolute timing.[20] In addition, the absorption models can benefit by better experimental characterization of these foils (e.g., a density measurement as a function of time). In this manner the plasma conditions obtained with the hydrodynamic calculations can be tested since the absorption models would be much more constrained. As a result, errors in the predicted temperature, if any, could be quantified.

Finally, there exists the temptation to correlate an average ionization charge, Z^*, with a given spectrum. As suggested by Abdallah *et al.*,[6,19] there are potential dangers in that assumption. Calculations of Z^* with and without the Coulomb corrections at the conditions of Table 1 show the largest difference to be less than 0.2 electrons. Such a small difference in Z^*, however, translates to a considerable difference in temperature (see Fig. 1). In addition, Z^* is not uniquely defined; that is, different absorption models can give different Z^* but produce very similar spectra or *vice versa.* Consequently, Z^* is not an optimal variable to quantify the transmission spectra.

Acknowledgments - We gratefully recognize valuable discussions with J.M. Foster, T.S. Perry, P.A. Rosen, and R. Ward as well as thank them for the experimental and theoretical results. Thanks are also due to R. Doyas for a code that manipulates our photon absorption results into a compact table, T. Kelleher for a monochromatic absorption interpolation code, and R.W. Lee for reading the manuscript. Work performed under the auspices of the Department of Energy by Lawrence Livermore National Laboratory under contract W-7405-ENG-48.

TABLE 1

Temperature and density simulation results[14] for the aluminum foil as a function of time.

Time [ps]	T [eV]	ρ [g/cm^3]
200	0.4	2.137
300	1.7	2.010
400	3.2	2.498
500	7.5	2.146
600	14.8	1.304
700	22.6	0.684
800	44.7	0.305
900	63.4	0.215
1000	76.8	0.227
1200	83.7	0.133

TABLE 2

Same as a Table 1 but with a 10% reduction in drive temperature.[14]

Time [ps]	T [eV]	ρ [g/cm^3]
200	0.334	2.34
300	1.12	2.79
400	1.99	1.16
500	4.12	2.58
600	7.42	1.88
700	9.45	1.14
800	11.9	0.675
900	21.8	0.420
1000	37.3	0.229
1200	59.2	0.119

REFERENCES

1. T.S. Perry *et al.*, *Phys.Rev.Lett.* **67**, 3784(1991).
2. J.M. Foster *et al.*, *Phys.Rev.Lett.* **67**, 3255(1991).
3. P.T. Springer *et al.*, *Atomic Processes in Plasmas*, eds. E.S. Marman & J.L. Terry (AIP, New York, 1991) pg.78.
4. P.T. Springer *et al.*, *Phys.Rev.Lett.* **69**, 3735(1992).
5. S.J. Davidson *et al.*, *Appl.Phys.Lett.* **52**, 7(1988); S.J. Davidson *et al.*, *Laser Interaction with Matter*, eds. G. Velarde, E. Minguez, & J. Perlado (World Scientific,Singapore, 1989).
6. J. Abdallah and R.E.H. Clark, *J. Appl. Phys.* **69**, 1 (1991).
7. C.A. Iglesias, J.K. Nash, M.H. Chen, & F.J. Rogers, *JQSRT* **51**, 125(1994)
8. T.S. Perry *et al.*, *JQSRT* **51**, 273(1994).
9. I.P. Grant *et al.*, *Comp.Phys.Commun.* **21**, 207(1980); B.J. McKenzie *et al.*, *Comp.Phys. Commun.* **21**, 233(1980)
10. M.H. Chen, *Phys.Rev.* **A31**, 1449(1985).
11. K.N. Huang *et al.*, *At.Data Nuc.Data Tables* **18**, 243(1976).
12. F.J. Rogers, *Proceeding of the International School of Physics <<Enrico Fermi>> Course CXIII/ High Pressure Equations of State: Theory and Applications*, eds. S. Siezer and R.A. Ricci (North Holland, Amsterdam, 1991) pg.77.
13. C.A. Iglesias, F.J. Rogers, & B.G. Wilson, *Ap.J.* **397**, 717(1992).
14. J.M. Foster & P.A. Rosen, private communication.
15. Only accounts for the timing errors of the streaked x-ray crystal spectrometer.
16. Neither experimental or hydrocode results were made available at t=1100ps.
17. W. Dappen, *Rev.Mex.Astron.Astrof.* **23**, 141(1992).
18. F.J. Rogers & C.A. Iglesias, *GONG 1992: Seismic Investigation of the Sun and Stars*, ed. T.M. Brown (A.P.S. Conf. Ser., San Fransisco, California, 1993) Vol.42, pg. 155.

19 J. Abdallah, R.E.H. Clark, & J.M. Peek, *Phys.Rev.* **A44**, 4072(1991).

20. Ref. 8 had a Si foil at the hot end of the gold tube but was compromised by the SiO_2 aerogel.

FIGURE CAPTIONS

Fig.1 - Transmission spectra from OPAL/MCDF model at T=70eV (—) and T=76.8eV (- · -) as well as a calculation from a model without the Coulomb corrections at T=76.8eV (- - -). All 3 calculations used ρ=0.227g/cm^3. The theoretical transmission in this and all subsequent figures have been convolved with a Gaussian function to account for an experimental resolution of $\lambda/\Delta\lambda$=800.

Fig.2 - Comparison of experiment (—) and OPAL/MCDF model (- - -) at conditions in Table 1.

Fig.3 - Comparison of experiment and OPAL/MCDF model at 2 temperatures and single density.

Fig.4 - Comparison of experiment (—) and OPAL/MCDF model (- - -) using Table 1 where the theory has been displaced to later times by 100ps.

Fig.5 - Comparison of experiment (—) and OPAL/MCDF model (- - -) at conditions in Table 2.

Fig.6 - Comparison of experiment (—) and OPAL/MCDF model (- - -) using Table 2 where the theory has been displaced to earlier times by 100ps.

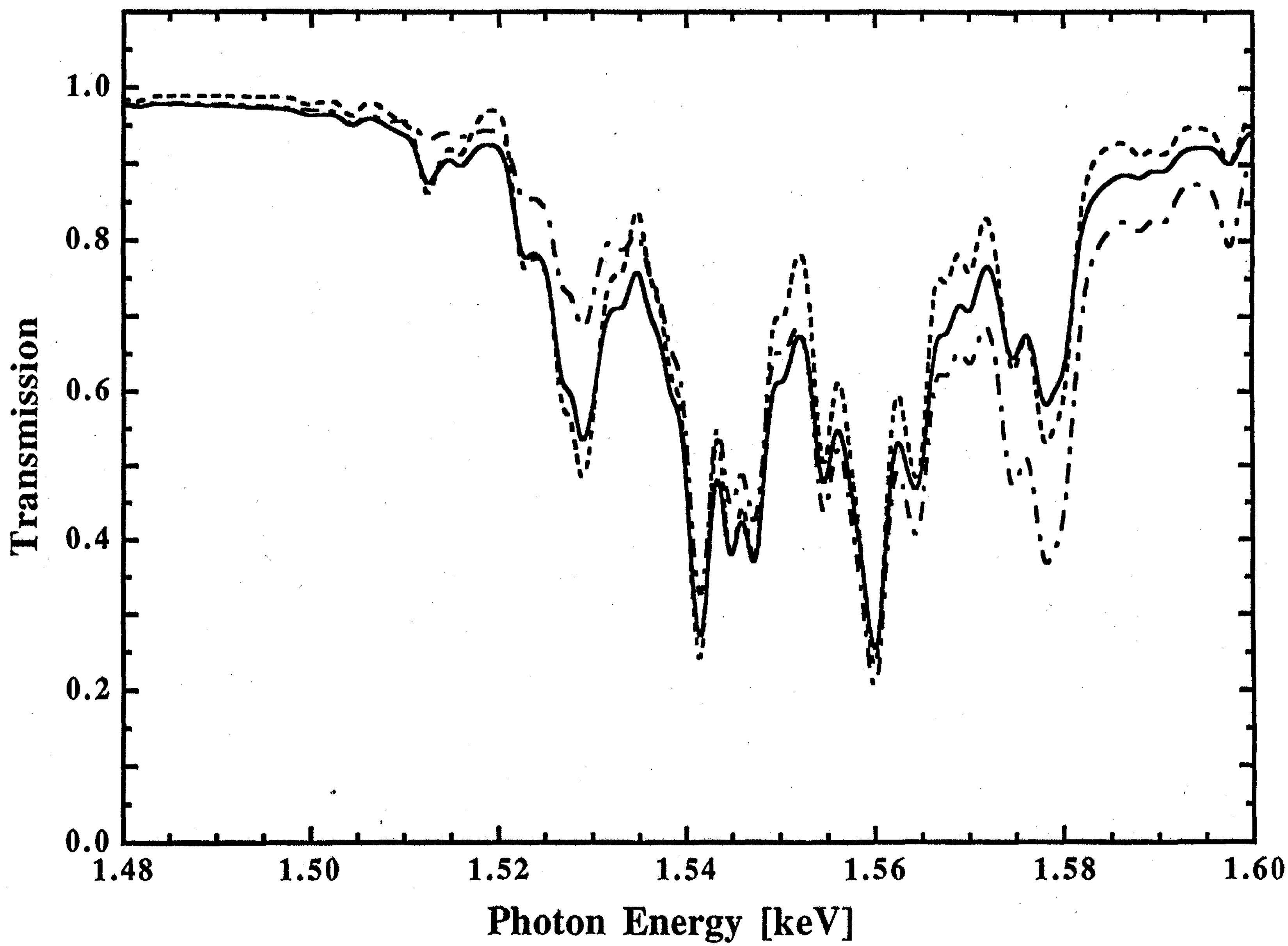
1.0
0.8
0.6
0.4
0.2
0.0
Transmission
1.48
1.50
1.52
1.54
1.56
1.58
1.60
Photon Energy [keV]

Fig. 1

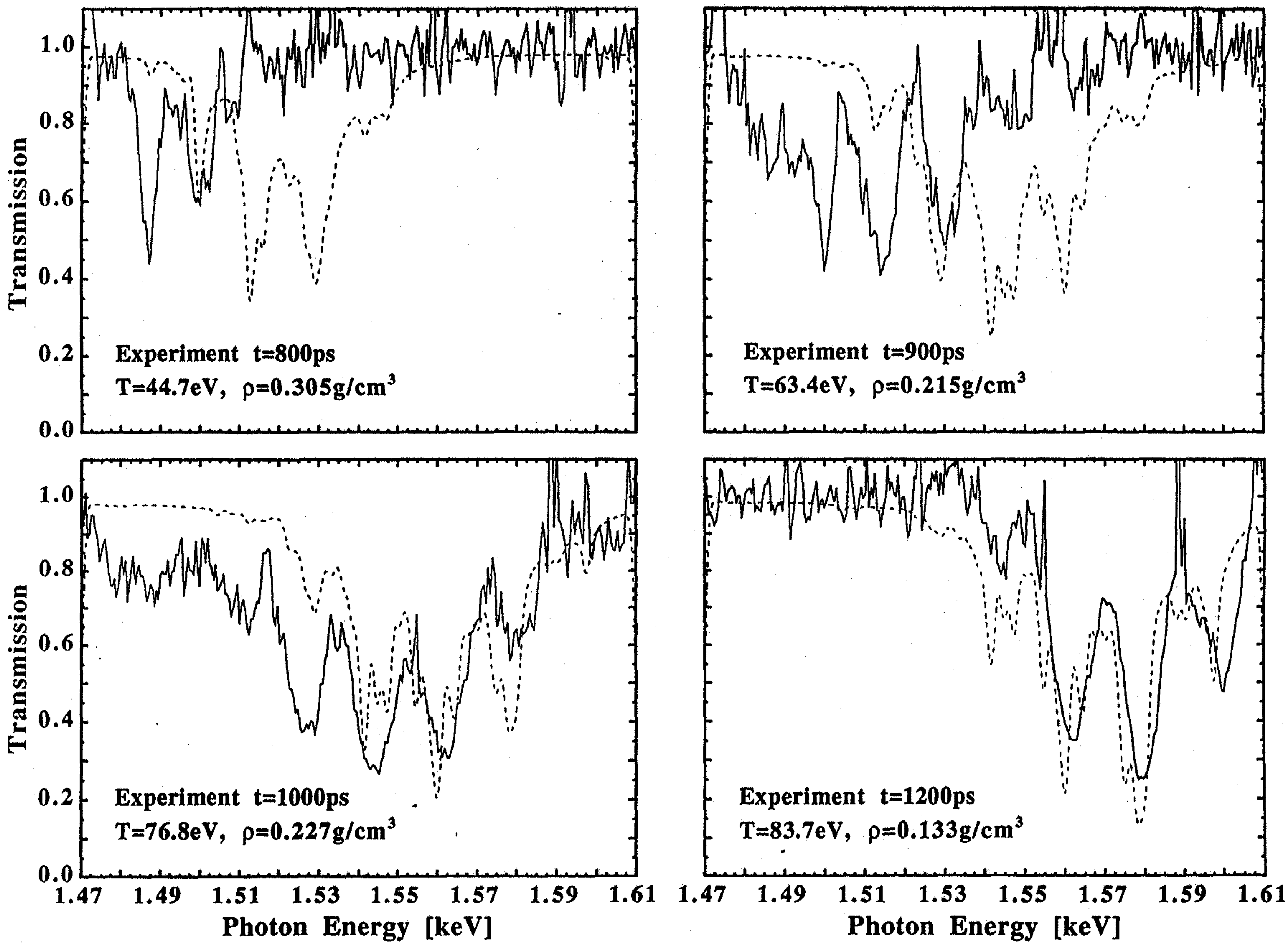
Transmission
Photon Energy [keV]
Experiment t=800ps
T=44.7eV, ρ=0.305g/cm³
Experiment t=900ps
T=63.4eV, ρ=0.215g/cm³
Experiment t=1000ps
T=76.8eV, ρ=0.227g/cm³
Experiment t=1200ps
T=83.7eV, ρ=0.133g/cm³
0.0
0.2
0.4
0.6
0.8
1.0
1.47
1.49
1.51
1.53
1.55
1.57
1.59
1.61

Fig. 2

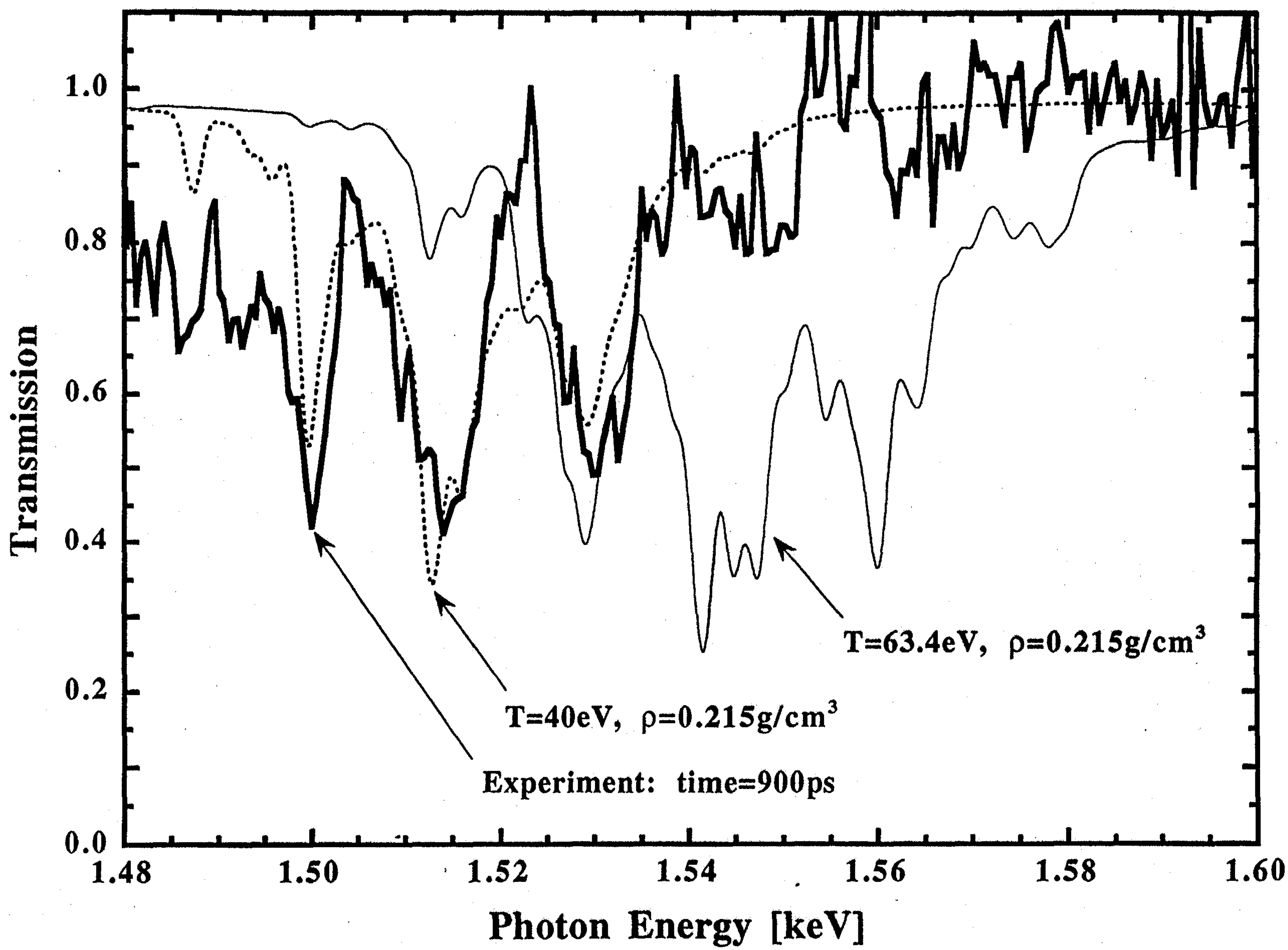
Transmission
1.0
0.8
0.6
0.4
0.2
0.0
1.48
1.50
1.52
1.54
1.56
1.58
1.60
Photon Energy [keV]
T=63.4eV, ρ=0.215g/cm3
T=40eV, ρ=0.215g/cm3
Experiment: time=900ps

Fig. 3

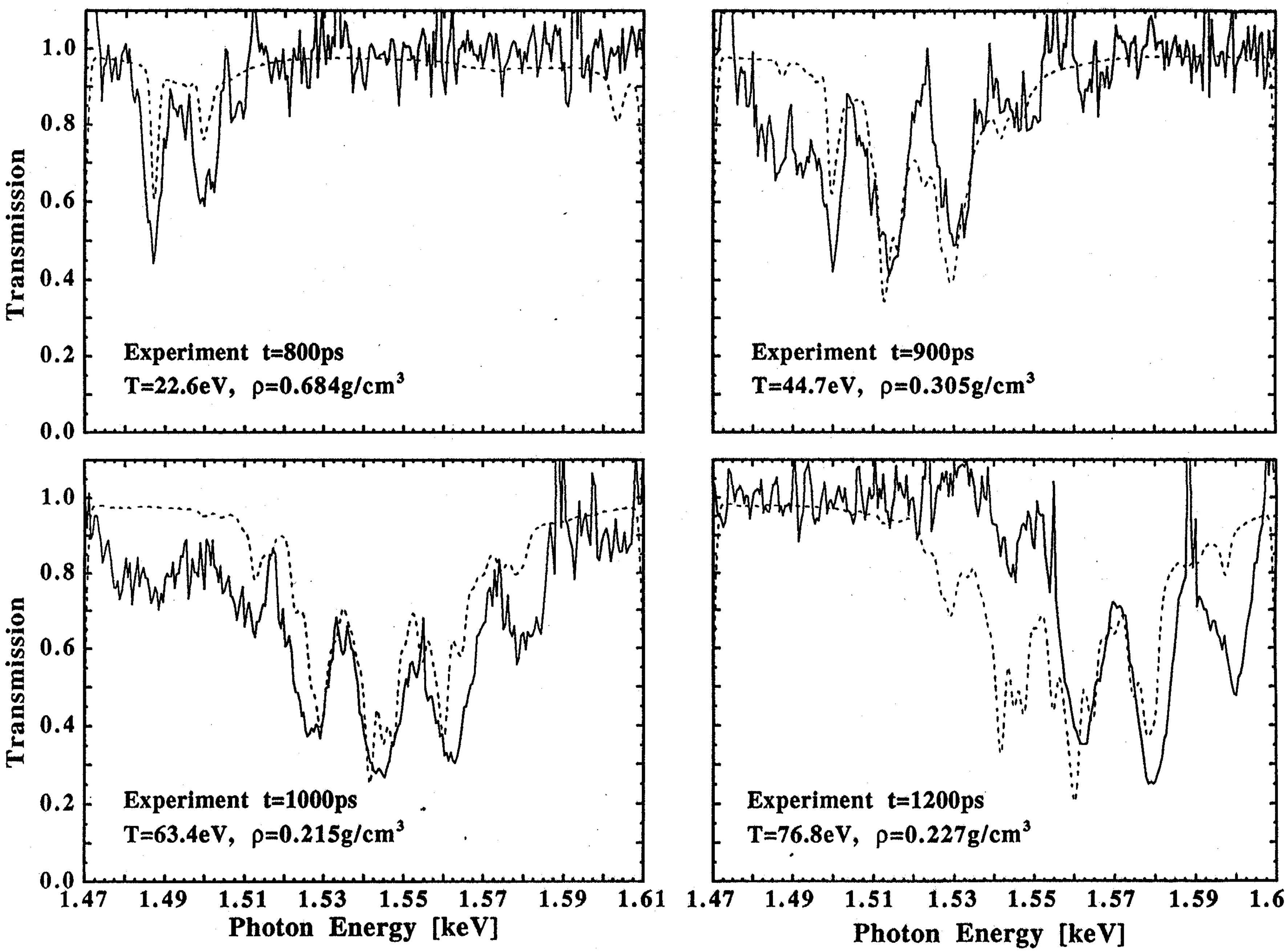
Transmission
1.0
0.8
0.6
0.4
0.2
0.0
Experiment t=800ps
T=22.6eV, ρ=0.684g/cm³
Experiment t=900ps
T=44.7eV, ρ=0.305g/cm³
Experiment t=1000ps
T=63.4eV, ρ=0.215g/cm³
Experiment t=1200ps
T=76.8eV, ρ=0.227g/cm³
1.47 1.49 1.51 1.53 1.55 1.57 1.59 1.61
Photon Energy [keV]

Fig. 4

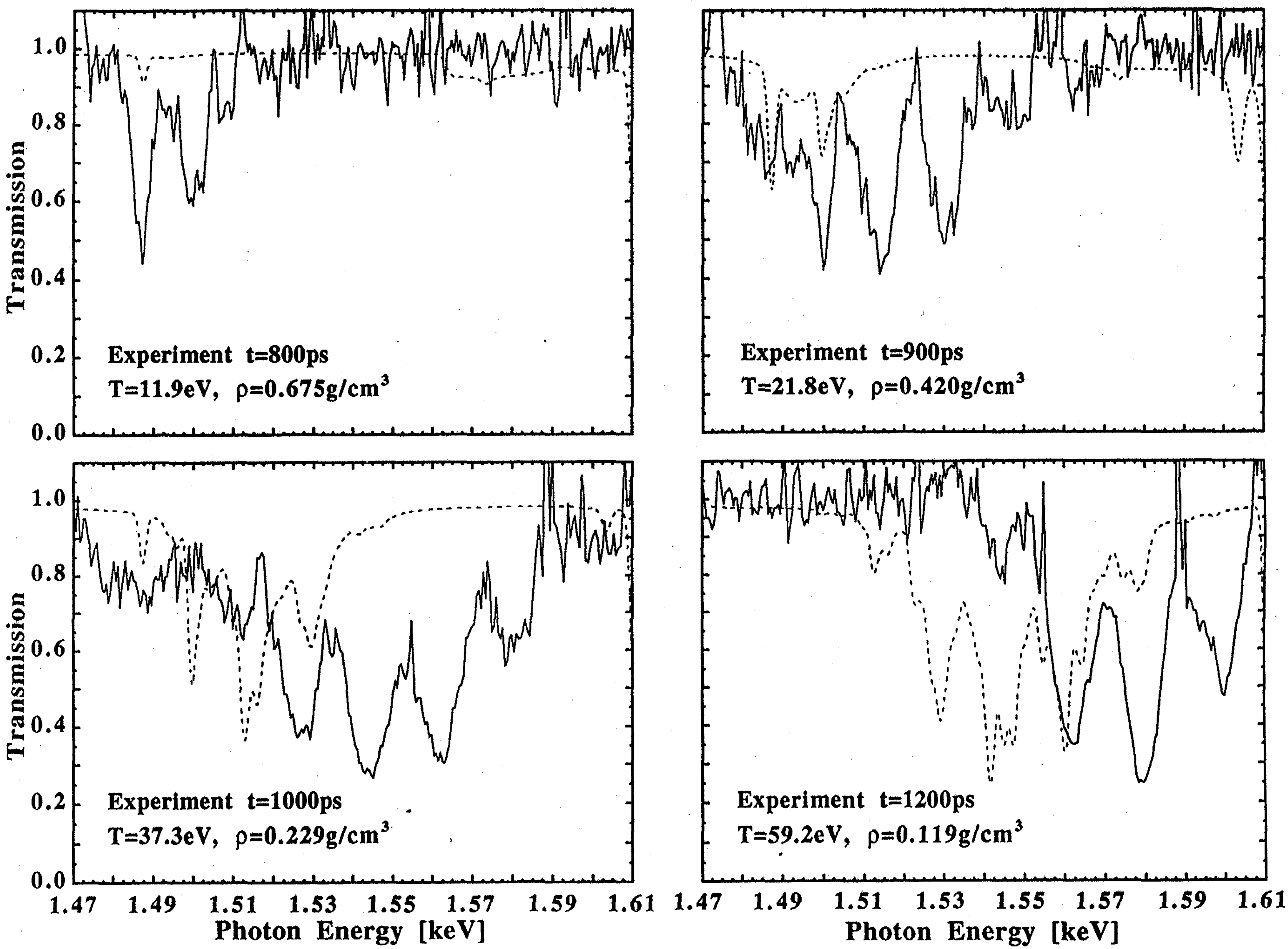
Transmission
1.0
0.8
0.6
0.4
0.2
0.0
Experiment t=800ps
T=11.9eV, ρ=0.675g/cm³
Experiment t=900ps
T=21.8eV, ρ=0.420g/cm³
Experiment t=1000ps
T=37.3eV, ρ=0.229g/cm³
Experiment t=1200ps
T=59.2eV, ρ=0.119g/cm³
1.47 1.49 1.51 1.53 1.55 1.57 1.59 1.61
Photon Energy [keV]

Fig. 5

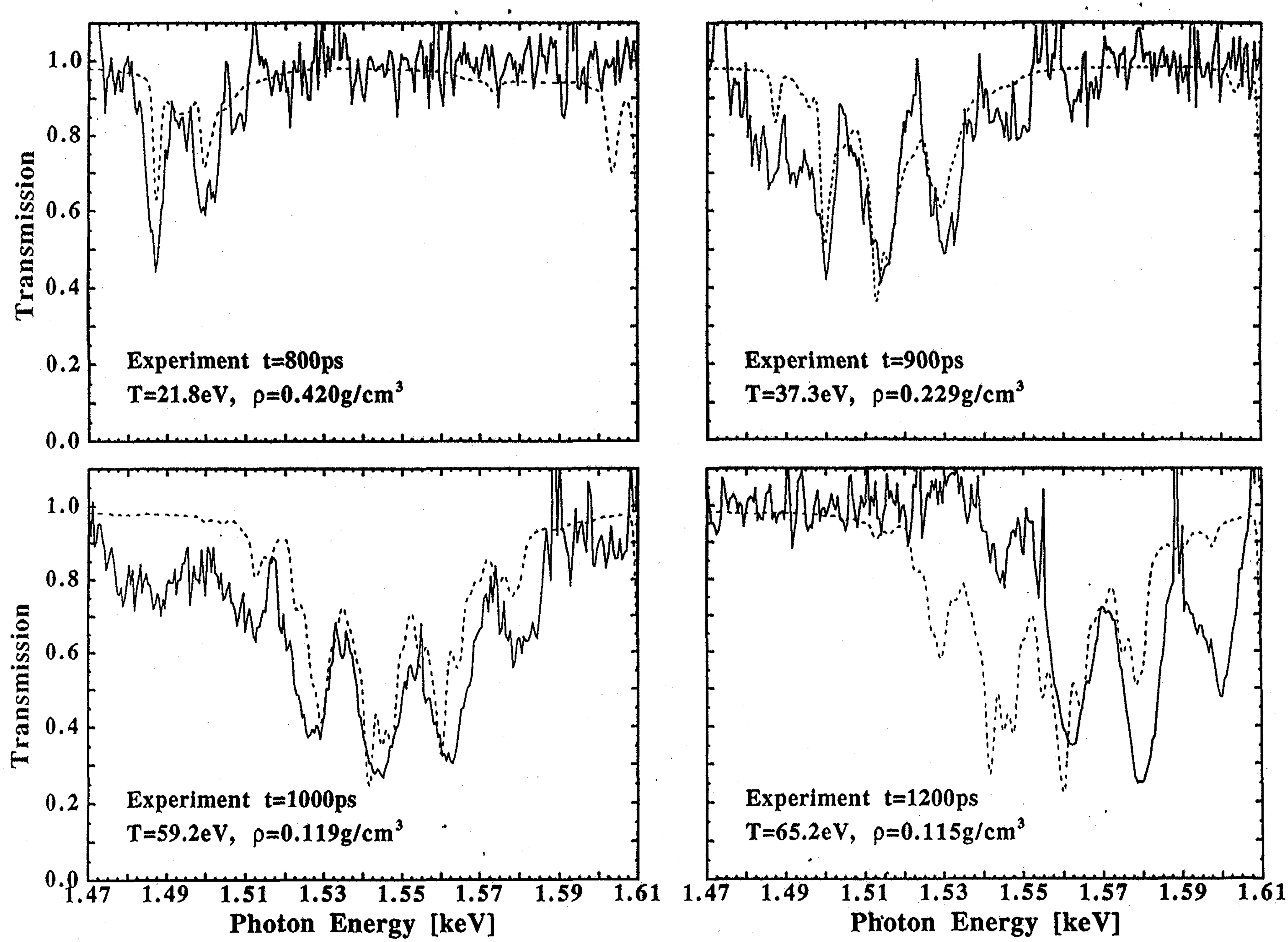

Transmission
1.0
0.8
0.6
0.4
0.2
0.0
Experiment t=800ps
T=21.8eV, ρ=0.420g/cm³
Experiment t=900ps
T=37.3eV, ρ=0.229g/cm³
Experiment t=1000ps
T=59.2eV, ρ=0.119g/cm³
Experiment t=1200ps
T=65.2eV, ρ=0.115g/cm³
1.47 1.49 1.51 1.53 1.55 1.57 1.59 1.61
Photon Energy [keV]

Fig. 6